

Replacing PET Plastic With PLA As A Sustainable Alternative To Functional Drink Containers

Camila Canturin, Alessandra Rojas and Rafael Villanueva

Industrial Engineering Department

Universidad de Lima

Lima, Perú

20200392@aloe.ulima.edu.pe, 20201838@aloe.ulima.edu.pe,

rvillan@ulima.edu.pe

Abstract

Polyethylene terephthalate (PET) is a widely used material in container manufacturing, particularly in bottle production. It is characterized by its low cost and widespread availability. However, its improper disposal has significantly exacerbated global plastic pollution. For instance, less than 50% of plastic bottles are recycled. Moreover, studies indicate that this issue has led to a significant accumulation of plastic waste in the oceans, which continues to grow annually and could be considered floating islands of debris. This study proposes replacing PET with polylactic acid (PLA), a biodegradable and biocompatible polymer with suitable properties for bottle production. PLA also has a shorter decomposition time compared to PET, contributing to the reduction of carbon footprint and greenhouse gas emissions. The research methodology included a diagnostic phase to define objectives, identify constraints, and determine variables based on an extensive literature review. The design phase focused on modeling a PLA-based bottle with detailed specifications and innovative structural features. Additionally, experimental evaluations of biodegradability, compressive strength, and tensile strength were conducted to compare PET and PLA. The study incorporated technical standards and engineering protocols to evaluate critical properties such as material permeability and stress behavior. As a result, it was confirmed that PLA exhibits properties that make it a competitive material compared to PET. In conclusion, this research presents a technically viable alternative to PET bottles through the use of PLA, with the potential to significantly mitigate environmental impacts while maintaining the functional requirements of packaging.

Keywords

PLA, PET, Biodegradability, Bottle and Properties

1. Introduction

The issue arising from global plastic production is its inadequate management. As evidence of this, only 20% of produced plastic bottles are recycled (Georgiou et al. 2022). Additionally, approximately 2.40 million tons of plastic waste are dumped into the ocean worldwide. According to Alhazmi, Almansour, and Aldhafeeri, this accumulation of 2.40 million tons of waste in the ocean has led to the creation of “The Great Pacific Garbage Patch” (as cited in Ajaj et al. 2022, p. 5). Furthermore, due to the inadequate disposal of PET bottles and their long-term persistence, CO₂ emissions are generated, leading to respiratory problems and an increase in global warming. Additionally, ecosystems are deteriorating, aquatic and terrestrial organisms are impacted, mosquito reproduction is encouraged, and various diseases affecting public health are proliferating (Ajaj et al. 2022). To mitigate these environmental impacts, solutions such as “Smart Use of Materials” (Suarez et al. 2022) and “material efficiency” (Pomponi et al. 2022) have been proposed, focusing on the intelligent use of materials and improved packaging design. For this reason, it is proposed to replace PET with a biodegradable material suitable for beverage packaging, such as PLA.

1.1 Objectives

The general objective of this study is to assess the technical, and environmental feasibility of replacing PET plastics with PLA plastics in functional beverage packaging as a sustainable alternative. Concerning the specific objectives, these are outlined below:

Characterize the physical and chemical properties of PET and PLA bottles to determine their suitability for functional beverage containment.

Design and conduct controlled laboratory experiments to evaluate the performance and durability of PLA and PET plastics under various conditions relevant to packaging.

2. Literature Review

The growing concern over plastic waste highlights the need for sustainable alternatives in packaging. Alarmingly, only 2% of plastic packaging is recycled into new products, with the rest ending up in landfills, being incinerated, or polluting natural environments (Phelan et al. 2022). On a global scale, approximately 70% of plastic packaging is discarded, specifically, 88.2 million tons of plastic waste annually (Soong et al. 2022). This inefficiency is further compounded by health concerns, as studies show that 80% of microplastics in bottled water stem from PET bottles, leading to an estimated annual intake of up to 90,000 particles per person (Kannan & Vimalkumar 2021). These statistics emphasize the urgent need for alternatives like polylactic acid (PLA). PLA stands out as a biopolymer derived from renewable biomass, offering biodegradability, biocompatibility, and superior mechanical properties, including a high elastic modulus and transparency (Arrieta et al. 2014). Additionally, its production process generates significantly lower greenhouse gas (GHG) emissions—only 11.85 kg CO₂eq per equivalent mass, compared to 498 kg CO₂eq for PET (Mohammed et al. 2023). These attributes make PLA particularly suitable for short-shelf-life food packaging, where its ease of processing and cost-efficiency are advantageous (Oliveira et al. 2022). Furthermore, the production of PLA still accounts for substantial environmental impacts, including contributions to acidification (40%), climate change (60%), and fossil fuel depletion (77%) (Moretti et al. 2021). Moreover, the environmental benefits remain notable, as the production of PLA bottles results in significantly lower ecotoxicity levels 88.26% less than that of PET (Bałdowska-Witos et al. 2020). While PLA offers a promising solution for reducing the environmental footprint of packaging, challenges remain in optimizing its production process and scaling its application. Its potential as a sustainable alternative underscores the importance of continued innovation and investment in circular economy strategies to mitigate the global plastic waste crisis.

3. Methods

The experimental methodology was selected to evaluate the material properties, comprising five key tests: Opacity and light transmittance, compression, tensile strength, chemical composition and biodegradability.

For the opacity and light transmittance tests, the requirements of ASTM D1003 were followed, which recommends at least three samples per material type to ensure result averaging and improve accuracy. The samples should be 50 mm in diameter or equivalent in square form (ASTM International 2000). Therefore, 3 x 3 cm samples were used for the test. The Shimadzu UV-VIS spectrophotometer UV-2600 from the Docimology Laboratory at the University of Lima was employed for the analysis. For the compression test, two references were used: ASTM D695 and the research article “Behaviour of sand-filled plastic bottled clay panels for sustainable homes” by Kim et al. (2019). ASTM D695 specifies that for isotropic materials, at least five specimens should be tested, excluding and replacing any defective or fractured samples (ASTM International 2010). In Kim et al.'s study, compression tests were conducted on 500 ml PET bottles, suggesting an ideal test range of 8 to 12 specimens (Kim et al. 2019). Accordingly, 10 bottles were selected for the test, meeting the threshold of five samples as per ASTM D695.

The test was conducted on the Tensometric X500-50 universal testing machine at the Metrology and Material Control Laboratory at the University of Lima, with a test speed of 20 mm/min until a displacement of approximately 70 mm was reached. With respect to the tensile strength test, ASTM D638 was applied, specifying the number of samples based on the material type. For isotropic materials, a minimum of five specimens is required, sized according to the thickness of the plastic being evaluated. For Type V specimens, ASTM D638 provides three test speeds (1, 10, and 100 mm/min); the standard recommends selecting a speed that causes failure within a range of 30 seconds to 5 minutes. Samples exhibiting defects, deformations, or breakages outside the gauge section (G) at the sample center must be discarded (ASTM International 2014). The tests were performed using the same equipment as in the compression test. The equipment was calibrated and set to a speed of 1 mm/min for 10 PLA and PET samples. Additionally, paper was applied to the ends of the samples to enhance grip during testing. With regard to the chemical composition analysis, ASTM E1252 was followed, which outlines several techniques for solid sample analysis using spectrophotometry.

One prescribed method involves grinding the sample into powder, compacting it into a pellet to ensure uniform distribution, thus enabling accurate spectral analysis of the material's chemical components (ASTM International 2021). Although ASTM E1252 does not specify an exact sample quantity, it requires sufficient powder contact with the crystal for reliable reading. For this, 10 PLA bottles and 12 PET bottles were ground. The grinding process was performed using a blade mill in the Operations and Unit Processes Laboratory at the University of Lima. The analysis was carried out using an FTIR spectrophotometer model IRTracer-100 in the Environmental Engineering Laboratory at the University of Lima, configured for 32 scans with a resolution of 2 cm^{-1} . For the biodegradability test, the ASTM D5338 guidelines were followed, which stipulate the use of compost inoculum, distilled water, plastic specimens, and containers. The standard prescribes 12 containers, distributed as follows: 3 with plastic and compost, 3 with compost only, 3 with biodegradable material and compost, and 3 with non-biodegradable material and compost (ASTM 2015). Due to laboratory constraints, the test conditions were adjusted based on the resources available in the Microbiology Laboratory at the University of Lima. Three containers were used: the first containing mushroom cultivation substrate with PLA fragments, the second containing substrate and PET fragments, and the third containing substrate only. These three containers were placed in a Precision Scientific BOD incubator at 50°C for 6 days, with measurements taken every 12 hours. It is worth noting that this temperature is the maximum setting of the incubator, and the duration of the experiment was determined based on the availability of the equipment.

4. Data Collection

The collected information on relevant aspects of the opacity and light transmittance, compression, tensile, chemical composition, and biodegradability tests is presented. Regarding the transmittance test, it measures the amount of light that passes through a material (ASTM International 2000). It is important to highlight that increased crystallinity enhances the material's resistance to UV rays, which can trigger a chain reaction leading to material degradation. While many plastics do not directly absorb radiation, impurities within the material can absorb it, breaking polymer chains and making the material brittle (Zeus 2019). In the compression and tensile tests, the mechanical behavior of the material is assessed. For example, density is related to the weight of the bottle per unit volume; a higher value means the bottle is heavier, which can affect transport and handling. The modulus of elasticity indicates the material's rigidity: a higher modulus means the material will resist deformation under load more effectively. The yield stress represents the maximum stress the material can withstand before permanent deformation occurs; therefore, a higher yield strength indicates better resistance to irreversible deformation.

Finally, the peak stress refers to the maximum stress the material can withstand before failure, indicating the material's ultimate resistance to fracture. Regarding chemical composition analysis, techniques such as spectroscopy are used to identify functional groups that influence the material's macroscopic properties. Finally, regarding the biodegradability test, a study evaluated the decomposition of the material after anaerobic treatment. The results showed that after 100 days, the material developed cracks and easily disintegrated (Zaborowska, M., 2021). In contrast, PET, a polymer derived from petroleum, is known for its intrinsic chemical stability, preventing rapid decomposition in the environment. PET is estimated to take between 400 and 500 years to decompose, significantly contributing to the accumulation of plastic waste (Gambino et al. 2020; Aslani et al. 2021).

5. Results and Discussion

5.1 Numerical Results

Regarding the compression test of the PET bottles, as shown in Figure 1, the maximum force applied was recorded in PET-9, with a value of 273.10 N, while the minimum was recorded in PET-5, with a value of 76.10 N. Regarding the cross-sectional area, a standard deviation of 24.130 mm was obtained, indicating low variability considering an average of 2975.26 mm. The posterior diameter remained relatively constant, with a standard deviation of less than 0.5 mm. The average density was 24.84 kg/m^3 . In terms of the elastic modulus, the minimum value was 0.219 N/mm^2 in PET-4, and the maximum was 4.092 N/mm^2 in PET-5, indicating that the latter exhibits greater stiffness. For the yield stress, the highest value was observed in PET-10, with 0.021 N/mm^2 , while PET-2 demonstrated lower resistance before permanent deformation. Regarding the peak stress, the highest value was 0.091 N/mm^2 in PET-9.

| Test N° | Peak force (N) | Area (mm ²) | Breadth (mm) | Density (kg/m ³) | Young's Modulus (N/mm ²) | Yield stress (N/mm ²) | Peak stress (N/mm ²) |
|-------------------|----------------|-------------------------|---------------|------------------------------|--------------------------------------|-----------------------------------|----------------------------------|
| PET - 1 | 68.100 | 2975.404 | 61.550 | 24.890 | 3.747 | 0.017 | 0.023 |
| PET - 2 | 99.000 | 2970.572 | 61.500 | 24.835 | 3.746 | 0.012 | 0.033 |
| PET - 3 | 252.900 | 2979.273 | 61.590 | 24.778 | 0.260 | 0.019 | 0.085 |
| PET - 4 | 245.900 | 3011.284 | 61.920 | 24.436 | 0.219 | 0.020 | 0.082 |
| PET - 5 | 76.100 | 3011.284 | 61.920 | 24.358 | 4.092 | 0.020 | 0.025 |
| PET - 6 | 100.900 | 2954.172 | 61.330 | 24.829 | 3.852 | 0.019 | 0.034 |
| PET - 7 | 226.200 | 2949.357 | 61.280 | 25.189 | 0.542 | 0.018 | 0.077 |
| PET - 8 | 226.000 | 2958.027 | 61.370 | 24.749 | 0.963 | 0.018 | 0.076 |
| PET - 9 | 273.100 | 2995.742 | 61.760 | 24.831 | 0.572 | 0.020 | 0.091 |
| PET - 10 | 220.400 | 2947.432 | 61.260 | 25.462 | 0.361 | 0.021 | 0.075 |
| MEAN | 178.860 | 2975.255 | 61.548 | 24.836 | 1.835 | 0.018 | 0.060 |
| S.D | 81.873 | 24.130 | 0.249 | 0.320 | 1.756 | 0.003 | 0.028 |
| C. of Var. | 0.458 | 0.008 | 0.004 | 0.013 | 0.957 | 0.138 | 0.459 |

Figure 1. PET compression test results

Regarding the compression test of the PLA bottles, the results are shown in Figure 2. The maximum force applied was recorded in PLA-9, with a value of 323.40 N, while the minimum was observed in PLA-10, with a value of 200.80 N. Regarding the cross-sectional area, a standard deviation of 21.04 mm was obtained, indicating low variability considering an average of 2793.55 mm. The posterior diameter remained relatively constant, with a standard deviation of less than 0.5 mm. The average density was 44.57 kg/m³. For Young's modulus, the minimum value was 6.851 N/mm² in PLA-4, while the maximum value was 11.465 N/mm² in PLA-1. For the yield stress, the highest value was 0.115 N/mm² in PLA-9, indicating that this material can withstand higher stresses before experiencing permanent deformation. Regarding the peak stress, the highest value was also 0.115 N/mm² in PLA-9.

| Test N° | Peak force (N) | Area (mm ²) | Breadth (mm) | Density (kg/m ³) | Young's Modulus (N/mm ²) | Yield stress (N/mm ²) | Peak stress (N/mm ²) |
|-------------------|----------------|-------------------------|---------------|------------------------------|--------------------------------------|-----------------------------------|----------------------------------|
| PLA - 1 | 209.400 | 2,795.480 | 59.660 | 44.482 | 11.465 | 0.034 | 0.075 |
| PLA - 2 | 318.000 | 2,791.733 | 59.200 | 44.650 | 9.126 | 0.114 | 0.114 |
| PLA - 3 | 294.500 | 2,759.982 | 59.280 | 45.195 | 8.307 | 0.079 | 0.107 |
| PLA - 4 | 268.100 | 2,812.374 | 59.840 | 44.307 | 6.851 | 0.053 | 0.095 |
| PLA - 5 | 276.000 | 2,756.259 | 59.240 | 45.004 | 7.535 | 0.098 | 0.100 |
| PLA - 6 | 202.000 | 2,810.494 | 59.820 | 44.260 | 10.695 | 0.072 | 0.072 |
| PLA - 7 | 291.900 | 2,797.355 | 59.680 | 44.623 | 9.396 | 0.104 | 0.104 |
| PLA - 8 | 270.200 | 2,786.116 | 59.560 | 44.647 | 7.068 | 0.097 | 0.097 |
| PLA - 9 | 323.400 | 2,814.254 | 59.860 | 44.231 | 8.736 | 0.115 | 0.115 |
| PLA - 10 | 200.800 | 2,811.434 | 59.830 | 44.291 | 10.460 | 0.071 | 0.071 |
| MEAN | 265.430 | 2793.548 | 59.597 | 44.569 | 8.964 | 0.084 | 0.095 |
| S.D | 46.129 | 21.040 | 0.265 | 0.327 | 1.574 | 0.027 | 0.017 |
| C. of Var. | 0.174 | 0.008 | 0.004 | 0.007 | 0.176 | 0.319 | 0.176 |

Figure 2. PLA compression test results

Based on the results obtained for both materials, the following conclusions can be drawn. The PLA bottles exhibited a higher Young's modulus, yield stress, and peak stress, indicating greater resistance to initial deformation, the ability to withstand higher stresses before undergoing permanent deformation, and a higher tension before reaching their maximum resistance compared to the PET bottles. However, the PLA bottles showed more dents and fractures than the PET bottles. This can be attributed to their lower ductility and a more brittle fracture mechanism. Additionally, the molecular chain orientation in PLA may be less favorable for resisting deformation in the direction of the applied load compared to PET. It is also important to note that the average cost of the test was \$20.56, and it was conducted on August 28th and 29th.

In the tensile test, the results were analyzed to evaluate key performance indicators. Initially, 10 samples were tested; however, due to machine configuration issues, several outliers were detected. As a result, the analysis was refined to focus on 6 samples. As shown in Figure 3, the lowest peak force was 50.50 N, observed in PET-5, while the highest was 65.20 N in PET-4. Furthermore, the peak stress varied, with a minimum of 13.80 N/mm² in PET-3 and a maximum of 18.63 N/mm² in PET-4. Finally, Young's modulus recorded its lowest value of 532.68 N/mm² in PET-2 and its highest value of 780.90 N/mm² in PET-6.

| Test N° | Peak force (N) | Peak stress (N/mm ²) | Young's modulus (N/mm ²) |
|-------------------|-------------------|-------------------------------------|---|
| PET - 2 | 58.600 | 16.740 | 532.680 |
| PET - 3 | 48.300 | 13.800 | 604.600 |
| PET - 4 | 65.200 | 18.630 | 581.280 |
| PET - 5 | 50.500 | 14.430 | 564.540 |
| PET - 6 | 59.800 | 17.090 | 780.900 |
| PET - 7 | 57.700 | 16.490 | 557.050 |
| MEAN | 56.683 | 16.197 | 603.508 |
| S.D | 6.252 | 1.787 | 90.174 |
| C. of Var. | 0.110 | 0.110 | 0.149 |

Figure 3. PET tensile test results

As shown in Figure 4, the lowest peak force was 102.60 N in PLA-4, while the highest was 162.20 N in PLA-5. Moreover, the peak stress varied from 4.69 N/mm² in PLA-4 to 7.41 N/mm² in PLA-5. Young's modulus also showed significant variation, with the lowest value of 190.03 N/mm² recorded in PLA-9 and the highest value of 262.24 N/mm² in PLA-5.

| Test N° | Peak force (N) | Peak stress (N/mm ²) | Young's modulus (N/mm ²) |
|-------------------|-------------------|-------------------------------------|---|
| PLA - 3 | 120.000 | 5.479 | 190.880 |
| PLA - 4 | 102.600 | 4.685 | 191.940 |
| PLA - 5 | 162.200 | 7.406 | 262.240 |
| PLA - 6 | 132.400 | 6.046 | 210.540 |
| PLA - 7 | 127.700 | 5.831 | 198.880 |
| PLA - 9 | 114.100 | 5.210 | 190.030 |
| MEAN | 126.500 | 5.776 | 207.418 |
| S.D | 18.610 | 0.850 | 25.507 |
| C. of Var. | 0.147 | 0.147 | 0.123 |

Figure 4. PLA tensile test results

Based on the results obtained for both materials, the following conclusions can be drawn. Although PLA shows higher resistance to maximum force compared to PET, it also exhibits lower rigidity and greater flexibility. This means that while PLA can withstand more force before breaking, it is more prone to deformation under moderate loads due to its flexibility. In contrast, PET, with greater rigidity, is better at resisting deformation but may be less capable of withstanding extreme forces without fracturing. In summary, PET is more resistant to deformation and behaves in a more rigid manner, while PLA, although stronger in terms of force resistance, is more flexible and less rigid. It is also important to mention that the cost of the test averaged \$6.17 and was conducted on September 5, 12 and 19.

5.2 Graphical Results

In this section, the results of transmission, biodegradability, and chemical composition tests will be interpreted. Additionally, an overview of the associated testing costs and scheduled dates will be presented to provide a comprehensive analysis of the feasibility and implementation timeline for these evaluations

Regarding the transmittance test, it refers to the amount of light passing through a material (ASTM International 2000). It is also important to note that higher crystallinity increases resistance to UV rays, which can trigger a chain reaction within the material leading to its degradation. Although many plastics do not absorb radiation, certain impurities can cause it by breaking the main polymer chains, making the material brittle (Zeus 2019). The test yielded transmittance percentages for different wavelength bands in nanometers. In Figure 5, the pink line represents PET material and the orange line represents PLA; indicating that PET exhibits lower light transmission with a maximum value of 89.76%, while PLA reaches 94.16%. This experiment was conducted on October 3rd in the Docimology Laboratory, with a total cost of \$6.17.

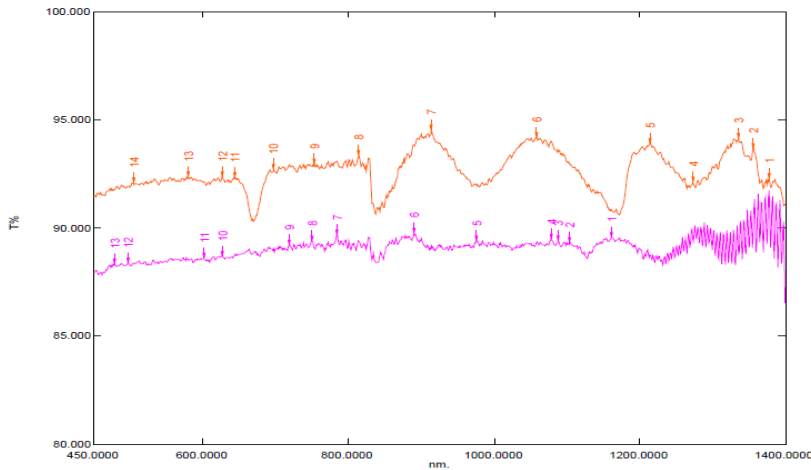


Figure 5. Transmittance analysis result

Regarding the biodegradability test, data were obtained from the software connected to the incubator. This software primarily provided the biochemical oxygen demand (BOD) in mg/L every 12 hours over 6.5 days. Due to an equipment issue, the duration of the experiment was shortened from the originally agreed 21 days; and had a total cost of \$15.93. The BOD was multiplied by 1 liter, the container's capacity, to obtain the BOD solely in mg.

To calculate the theoretical CO₂ evolution, the following preliminary calculations were performed. First, the approximate molar masses of each element were considered: Carbon (C) at 12 g/mol, oxygen (O₂) at 16 g/mol, and carbon dioxide (CO₂) at 44 g/mol. It should also be noted that, according to the material balance, all elements in the chemical equation contain 1 mole. Therefore, the conversion factor used was 44 g CO₂ / 32 g O₂ for each provided BOD value. From measurement 14 to 25, the theoretical CO₂ quantity remained constant as it exceeded the software limits. Figure 6 is presented to observe the increase in CO₂ quantity, indicating that PLA is being decomposed by organisms, such as bacteria, in a biodegradation process.

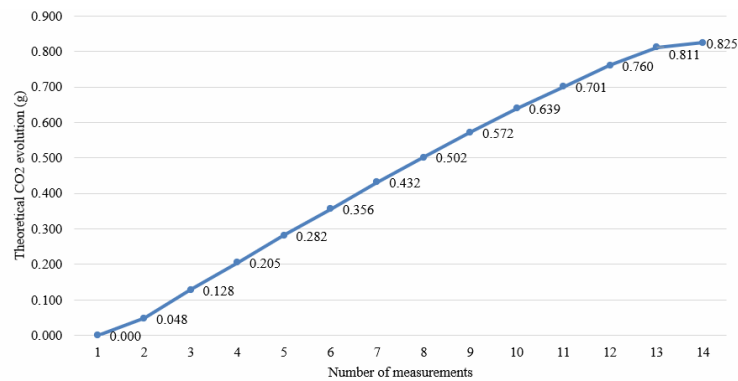


Figure 6. Theoretical CO₂ evolution

Figure 7 shows the biodegradation percentage of the material. This was calculated by dividing the difference between the final and initial BOD quantities by the final BOD. It is important to note that the indicator reflects a one-day period to standardize the results.

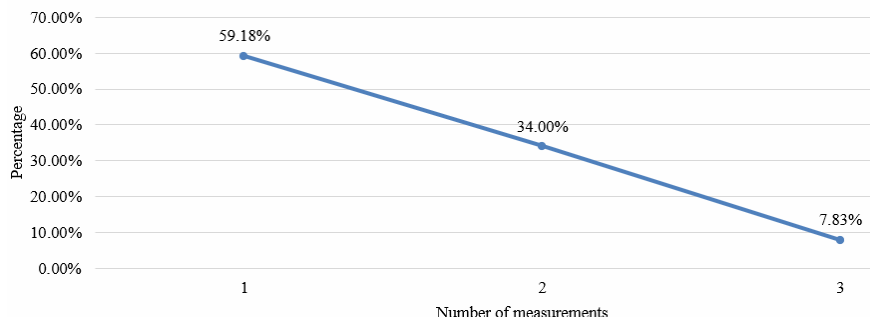


Figure 7. Biodegradation percentage

Regarding the chemical composition analysis using the IR spectrophotometer, the results are presented below in **Figure 8**. The test conditions included 32 scans and a resolution of 2 cm^{-1} with the model “RTracer-100_IRTracer100.” The test was conducted from September 4th to 12th in the microbiology laboratory, with a cost of \$2.06. In the graph, the peaks are characteristic of the functional groups of each material; the purple line represents PET, while the red line represents PLA.

In each spectral band, a characteristic “peak” is generated due to the percentage of transmittance (T%) exhibited by the material. Complementarily, the percentage of absorbance (Abs%) is calculated as the complement of the transmittance. This test enables the identification of functional groups within materials, which are indirectly related to their macroscopic properties.

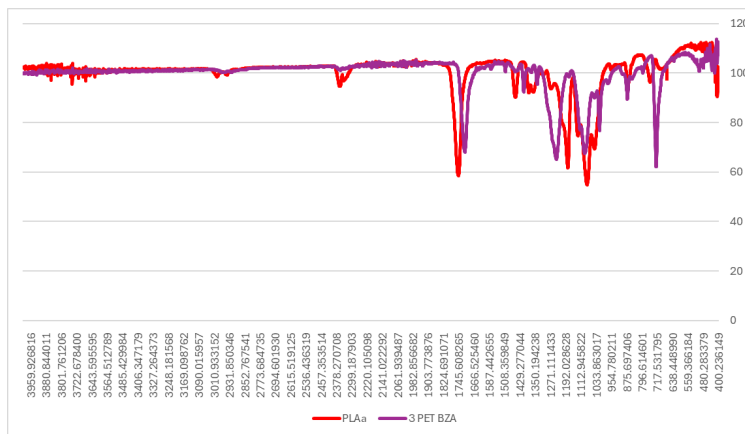


Figure 8. Composition analysis results

The first peak corresponds to the carbonyl (C=O) group in esters, notable for its highly polar bond and strong peak due to carbon-oxygen interactions (Miller 2022). Its double bond requires approximately 741 kJ/mol to break (LibreTexts n.d.). For PLA, the carbonyl peak is observed around 1750 cm^{-1} (Mofokeng et al. 2012), while for PET, it appears between 1700 cm^{-1} (Smith 2022) and approximately 1745 cm^{-1} (Venkatesulu et al. 2024), influenced by its aromatic ring. Chemical composition analysis confirmed peaks at approximately 1750 cm^{-1} for PLA and 1711 cm^{-1} for PET. While this functional group does not directly affect material properties, its double bond enhances structural rigidity and stability, as more energy is required to break the bond. In PLA, it also contributes to biodegradability through hydrolysis, where water molecules break polymer chains via nucleophilic attack (Gu et al. 2023). The second peak relates to the deformation of the C-H bond in PLA and aromatic ring stretching in PET. In PLA, this occurs at $1470\text{--}1450\text{ cm}^{-1}$ in the methylene (CH₂) group, known as “scissoring” deformation (LibreTexts n.d.), and in the methyl (CH₃) group as the “umbrella” mode (Beaucage n.d.). For PET, aromatic ring C-C bond stretching occurs within $1400\text{--}1500\text{ cm}^{-1}$ (LibreTexts n.d.). Experimental data showed peaks at 1450 cm^{-1} for PLA and 1411 cm^{-1} for PET. The third peak is associated with ester (C-O-C) stretching. For PLA, this appears at $1140\text{--}1070\text{ cm}^{-1}$ for saturated esters (Miller 2022). Mixed esters, with one aromatic carbon, show peaks at $1010\text{--}1050\text{ cm}^{-1}$ and $1200\text{--}1300\text{ cm}^{-1}$, with the aromatic ring causing higher frequency peaks (Miller 2022). According to LibreTexts (n.d.), this stretching

typically occurs within the 1000 - 1300 cm^{-1} range. PET peaks were observed at 1209 cm^{-1} and 1092 cm^{-1} , while PLA peaks appeared at 1180 cm^{-1} and 1080 cm^{-1} . Additionally, PET exhibits a unique peak at 720–730 cm^{-1} , linked to the methylene (CH_2) group due to ester-aromatic ring interactions (Socrates 2021; Pereira et al. 2017).

5.3 Proposed Improvements

The proposed improvements for the project include several adjustments to enhance testing accuracy and data representativeness.

In the biodegradability test, it is essential to consider both the composting inoculum’s operating temperature and the incubator’s maximum temperature, as some inoculums function at higher temperatures, such as 60°C, while the incubator in the Microbiology laboratory has a limit of 50°C, which restricts experiments under these conditions. Extending the incubation period for samples would allow observation of variations over several weeks, and incorporating oxygen and CO₂ sensors would provide more precise measurements. Using additional samples and containers in the biodegradability test would also enhance data robustness. For the tensile tests, it is recommended to use alternative types of grips on the X500-50 universal testing machine, as the small sample sizes led to measurement difficulties. Conducting these tests across a range of temperatures, from 14 to 30°C, is also advised, as the indicators do not show a proportional relationship with temperature. This approach would yield results that more accurately reflect the bottles' life cycle. Finally, for the chemical composition test, using alternative laboratory equipment would facilitate more efficient fine powder collection, as the current process requires multiple repetitions and allows only small quantities of powder to be extracted per cycle.

5.4 Validation

The biodegradability test aimed to achieve a degradation percentage of over 70% after a 45-day period (Moreno 2020). However, due to limited availability of the incubator housing the samples, the test was conducted over a 4-day period. During this time, daily measurements of biodegradation percentages were recorded for both PET and PLA. It is important to note that PET remained at 0% biodegradation, while PLA showed measurable variations, making it the primary focus of the analysis. To evaluate the results in comparison to the reference value, the variation in the biodegradation percentage between the value at the start of the final day and the value at the start of the second day was calculated. This period was selected because, after 12 hours on the final day, the Biochemical Oxygen Demand (BOD) reached 600 $\text{mg O}_2/\text{L}$ and stabilized due to system limitations. Therefore, for a more accurate assessment, the value recorded before this stabilization was used.

Specifically, the BOD at the beginning of the last day was 590 $\text{mg O}_2/\text{L}$, compared to 205 $\text{mg O}_2/\text{L}$ at the beginning of the second day, resulting in a calculated variation of 65.25%, as shown in Figure 9. Despite the test being limited to just 4 days, this result closely aligns with the expected reference value. Therefore, it can be inferred that the biodegradation percentage would likely increase with a longer test duration. These findings highlight the high biodegradability of PLA.

| Day | 1 | 2 | 3 | 4 | Biodegradability percentage variation |
|-------|---|-----|-----|-----|---------------------------------------|
| Start | 0 | 205 | 416 | 590 | 65.25% |

Figure 9. Biodegradation percentage variation

Regarding the transmittance test, the ASTM International (2000) standard, “Standard Test Method for Haze and Luminous Transmittance of Transparent Plastics,” specifies optimal total transmittance values between 90% and 99%. The results obtained in the test align with this standard, as the minimum and maximum values recorded were 88.24% to 89.76% for PET and 90.31% to 94.55% for PLA. Therefore, based on the results, both materials meet the established parameter, with PET demonstrating the highest level of performance, as shown in Figure 10.

| Material | Minimum | Maximum | Average | Expected percentage |
|----------|---------|---------|---------|---------------------|
| PET | 88.24% | 89.76% | 88.93% | 90% - 99% |
| PLA | 90.31% | 94.55% | 92.51% | |

Figure 10. Total transmission percentage

In addition, regarding the haze percentage values, according to the previously mentioned standard, the optimal haze range must be below 2%. Based on the results obtained in Figure 11, both materials meet the established parameter, with PET being the most optimal.

| Material | Diffuse transmission (%) | Total transmission (%) | Haze (%) | Expected percentage |
|----------|--------------------------|------------------------|----------|---------------------|
| PET | 1.26% | 89.93% | 1.40% | < 2% |
| PLA | 1.72% | 92.51% | 1.86% | |

Figure 11. Haze percentage

In relation to the compression test, the evaluated indicator is the yield stress (N/mm²). The values obtained for PET and PLA are presented below in Figure 12. In the case of PET, the yield strength is within the range of 20 to 107 N/mm² on average (MatWeb, 2024); however, the average value obtained is 0.018 N/mm². For PLA, the yield stress is considered close to the flexural elastic limit, which is at least 0.170 MPa (MatWeb, 2024). The obtained value is 0.084 N/mm². Therefore, in both cases, there are discrepancies compared to the reference data; however, the difference is more significant in the case of PET. This can be explained by the ambient temperature of 15°C and the loading rate of 20 mm/min.

| Test Nº | PET Stress Yield (N/mm ²) | PLA Stress Yield (N/mm ²) |
|------------|---------------------------------------|---------------------------------------|
| 1 | 0,017 | 0,034 |
| 2 | 0,012 | 0,114 |
| 3 | 0,019 | 0,079 |
| 4 | 0,020 | 0,053 |
| 5 | 0,020 | 0,098 |
| 6 | 0,019 | 0,072 |
| 7 | 0,018 | 0,104 |
| 8 | 0,018 | 0,097 |
| 9 | 0,020 | 0,115 |
| 10 | 0,021 | 0,071 |
| MEAN | 0,018 | 0,084 |
| S.D | 0,003 | 0,027 |
| C. of Var. | 0,138 | 0,319 |

Figure 12. Stress Yield

Regarding the results of the chemical composition, a summary table is presented that compares the spectral bands, where the presence of specific functional groups is expected, according to various authors, with the values obtained using the equipment. Figure 13 allows for verification that the measured values fall within the range proposed by these authors.

| Functional group | Sample | Expected band (cm-1) | Author | Spectrum (cm-1) | T (%) | Abs (%) |
|---|--------|----------------------------|--|--------------------|----------------|----------------|
| Carbonyl C=O | PLA | 1750 | (Mofokeng et al., 2012) | 1750.43 | 59.45 | 40.55 |
| | PET | 1700 - 1745 | (Smith, B.C, 2022) (Venkatesulu et al., 2024) | 1710.89 | 69.33 | 30.67 |
| C-H and stretching of the aromatic ring | PLA | 1470 - 1450 | (LibreTexts, s. f.) | 1450.49 | 90.37 | 9.63 |
| | PET | 1400 - 1500 | (LibreTexts, s. f.) | 1410.95 | 93.80 | 6.20 |
| Ester C-O-C | PLA | 1140 - 1070 | Miller (2022) | 1180.46 1080.16 | 61.53 55.02 | 38.47 44.98 |
| | PET | 1200 - 1300 | (Miller, 2022) | 1209.39 | 91.17 | 8.83 |
| | | 1010 - 1050 1000 - 1300 | (Miller, 2022) (LibreTexts, s. f.) | 1091.73 | 67.64 | 32.36 |
| Methylene CH2 deformation | PET | 720 - 730 | (Socrates, G., 2001) | 720.43 | 68.41 | 31.59 |

Figure 13. Spectrophotometer results

In relation to the tensile test, the evaluated indicators are the peak stress (MPa) and the elasticity modulus or Young's modulus (GPa) shown in Figure 14. The estimated values for PLA and PET are presented for a temperature range of 10 to 20°C, as the laboratory temperature is considered. Regarding peak stress (MPa), it ranges from 0.160 to 3000 MPa. It also varies from 5 to 42 MPa when the temperature is between 30 and 110°C. Therefore, a value below 5 MPa is considered. The obtained average value is 5.78 N/mm² or MPa, which meets the reference value.

As for the elasticity modulus (GPa), it ranges from 0.00232 to 13.8 GPa. It is specified that for a temperature range of 30 to 110°C, the value varies from 2.96 to 3.60 GPa. Therefore, a value below 2.96 GPa is considered. The obtained

average value is 207.42 MPa, which aligns with the estimated value (MatWeb, 2024). For PET, regarding peak stress (MPa), it ranges from 22 to 830 MPa. The obtained average value is 16.20 N/mm² or MPa, which does not meet the reference value. Regarding the elasticity modulus (GPa), it ranges from 1.57 to 5.20 GPa. The obtained average value is 603.51 MPa or 0.60351 GPa, which meets the estimated value.

| Material | PET | | PLA | | |
|----------|-------------------|----------------------------------|--------------------------------------|----------------------------------|--------------------------------------|
| | Test Nº | Peak stress (N/mm ²) | Young's modulus (N/mm ²) | Peak stress (N/mm ²) | Young's modulus (N/mm ²) |
| | 1 | 16.74 | 532.68 | 5.48 | 190.88 |
| | 2 | 13.8 | 604.6 | 4.69 | 191.94 |
| | 3 | 18.63 | 581.28 | 7.41 | 262.24 |
| | 4 | 14.43 | 564.54 | 6.05 | 210.54 |
| | 5 | 17.09 | 780.9 | 5.83 | 198.88 |
| | 6 | 16.49 | 557.05 | 5.21 | 190.03 |
| | MEAN | 16.197 | 603.508 | 5.778 | 207.418 |
| | S.D | 1.787 | 90.174 | 0.931 | 27.941 |
| | C. of Var. | 0.110 | 0.149 | 0.161 | 0.135 |

Figure 14. Peak stress and elasticity modulus

6. Conclusion

In this section, the conclusions of the present study are presented.

Regarding the properties of the materials studied, the following observations are made. PET is characterized by its hardness, high transparency, and adequate thermal resistance. However, it is derived from fossil sources, which results in slow decomposition. On the other hand, PLA is considered a material with lower hardness compared to PET, low impact resistance, and low permeability. Furthermore, it is produced from organic compounds, making it biodegradable. Under optimal conditions, it could degrade within 100 days.

Tensile, compression, light transmittance and opacity, chemical composition, and biodegradability tests were planned and conducted for both plastics. These tests were carried out in the laboratories of Metrology and Materials Control, Assaying, Microbiology, and Environmental Engineering. Moreover, each test was based on a specific standard. It is worth noting that the procedures were adapted to the availability of the equipment, and the suggestions of the laboratory staff were taken into consideration. Controlled laboratory experiments highlighted the key performance differences between PET and PLA under conditions relevant to beverage packaging. PET proved to be more resistant to deformation and maintained its integrity better under mechanical stress. PLA, despite its reduced mechanical performance, showed promising results in biodegradability tests, aligning with sustainability goals. Laboratory testing in University of Lima played a crucial role in evaluating the practical performance of PET and PLA, providing reliable data on their physical, chemical, and mechanical properties. These experiments allow for a thorough comparison of durability and biodegradability, helping to identify strengths and limitations of each material.

References

- Ajaj, R., Abu Jadayil, W., Anver, H., and Aqil, E., A revision for the different reuses of polyethylene terephthalate (PET) water bottles, *Sustainability (Switzerland)*, vol. 14, no. 8, 2022, Available: <https://doi.org/10.3390/su14084583>.
- Arrieta, M. P., López, J., Rayón, E., and Jiménez, A., Disintegrability under composting conditions of plasticized PLAePHB blends, *Polymer Degradation and Stability*, 2014, Available: <https://doi.org/10.1016/j.polymdegradstab.2014.01.034>.
- ASTM International, Standard Test Method for Haze and Luminous Transmittance of Transparent Plastics, 2000, Available: <https://file.yizimg.com/175706/2011120519401287.pdf>.
- ASTM International, Standard Test Method for Compressive Properties of Rigid Plastics, 2010, Available: <https://borgoltz.aoe.vt.edu/aoe3054/manual/expt5/D695.6642.pdf>.
- ASTM International, Standard Test Method for Tensile Properties of Plastics1, 2014, Available: <https://borgoltz.aoe.vt.edu/aoe3054/manual/expt5/D638.38935.pdf>.
- ASTM International, Standard Test Method for Determining Aerobic Biodegradation of Plastic Materials Under Controlled Composting Conditions, Incorporating Thermophilic Temperatures, 2015, Available: <https://cdn.standards.iteh.ai/samples/91521/fa456df9f80e4b4da25aace2a0fd2d75/ASTM-D5338-15.pdf>.
- ASTM International, Standard Practice for General Techniques for Obtaining Infrared Spectra for Qualitative Analysis, 2021, Available:

- <https://cdn.standards.iteh.ai/samples/108709/5193883377854da5876bf8770031315c/ASTM-E1252-98-2021-.pdf>.
- Baldowska-Witos, P., Kruszelnicka, W., Kasner, R., Tomporowski, A., Flizikowski, J., Klos, Z., Piotrowska, K., and Markowska, K., Application of LCA method for assessment of environmental impacts of a polylactide (PLA) bottle shaping, *Polymers*, vol. 12, no. 2, 2020, Available: <https://doi.org/10.3390/polym12020388>.
- Beaucage, G., Chapter 5: X-ray diffraction, University of Cincinnati, Available: <https://www.eng.uc.edu/~beaucag/Courses/Analysis/Chapter5.html>. Accessed on September 7, 2024.
- Georgiou, E. P., Drees, D., Lopes, L. M., and Gerlach, C., Measuring the frictional behavior and adhesion of PET bottles, *Lubricants*, vol. 10, no. 9, 2022, Available: <https://doi.org/10.3390/lubricants10090204>.
- Gu, Y., Bao, C., Zhang, S., Wang, H., and Zhao, Z., Mechanical properties of polymer composites reinforced with graphene oxide, *Polymer*, vol. 269, pp. 125679, 2023, Available: <https://doi.org/10.1016/j.polymer.2023.125679>.
- Kannan, K., and Vimalkumar, K., A review of human exposure to microplastics and insights into microplastics as obesogens, *Frontiers in Endocrinology*, vol. 12, 2021, Available: <https://doi.org/10.3389/fendo.2021.724989>.
- Kim, B., Wisniewski, J., Baker, T., and Oyinlola, M., Behaviour of sand-filled plastic bottled clay panels for sustainable homes, *Journal of Building Engineering*, vol. 25, 2019, Available: <https://doi.org/10.1016/j.jobe.2019.100895>.
- LibreTexts, Bond strength, LibreTexts, Available: https://chem.libretexts.org/Courses/Oregon_Tech_PortlandMetro_Campus/OT_-_PDX_-_Metro%3A_General_Chemistry_II/03%3A_Lewis_Structures/3.06%3A_Bond_Strength. Accessed on September 7, 2024.
- LibreTexts, Infrared spectra of some common functional groups, LibreTexts, Available: [https://chem.libretexts.org/Bookshelves/Organic_Chemistry/Map%3A_Organic_Chemistry_\(Wade\)_Complete_and_Semesters_I_and_II/Map%3A_Organic_Chemistry_\(Wade\)/11%3A_Infrared_Spectroscopy_and_Mass_Spectrometry/11.05%3A_Infrared_Spectra_of_Some_Common_Functional_Groups](https://chem.libretexts.org/Bookshelves/Organic_Chemistry/Map%3A_Organic_Chemistry_(Wade)_Complete_and_Semesters_I_and_II/Map%3A_Organic_Chemistry_(Wade)/11%3A_Infrared_Spectroscopy_and_Mass_Spectrometry/11.05%3A_Infrared_Spectra_of_Some_Common_Functional_Groups). Accessed on September 7, 2024.
- MatWeb, Overview of materials for Polyethylene Terephthalate (PET), Unreinforced, MatWeb, 2024, Available: <https://www.matweb.com/search/DataSheet.aspx?MatGUID=a696bdcdff6f41dd98f8ecc3599eaa20>.
- MatWeb, Overview of materials for Polylactic Acid (PLA) Biopolymer, MatWeb, 2024, Available: <https://www.matweb.com/search/DataSheet.aspx?MatGUID=ab96a4c0655c4018a8785ac4031b9278>.
- Miller, L., The infrared spectra of polymers. VII. Polymers with carbonyl (C=O) bonds, *Spectroscopy Online*, December 5, 2022, Available: <https://www.spectroscopyonline.com/view/the-infrared-spectra-of-polymers-vii-polymers-with-carbonyl-c-o-bonds>.
- Mofokeng, J. P., Luyt, A. S., Tabi, T., and Kovacs, J. G., Comparación de compuestos reforzados con fibras naturales moldeados por inyección con PP y PLA como matrices, *Journal of Thermoplastic Composite Materials*, 2012, Available: <https://doi.org/10.1177/0892705711433921>.
- Mohammed, A., Ward, K., Lee, K. Y., and Dupont, V., The environmental impact and economic feasibility assessment of composite calcium alginate bioplastics derived from Sargassum, *Green Chemistry*, vol. 25, no. 14, pp. 5501–5516, 2023, Available: <https://doi.org/10.1039/d3gc01019h>.
- Moreno Martinez, P., Estudio de la biodegradabilidad y compostabilidad de los diferentes plásticos, Repositorio Digital UPCT, Universidad Politécnica de Cartagena, 2020, Available: <https://repositorio.upct.es/server/api/core/bitstreams/e4956b4b-375b-41ff-be22-0fc3fb820adc/content>.
- Moretti, C., Hamelin, L., Jakobsen, L. G., Junginger, M. H., Steingrimsdottir, M. M., Høiby, L., and Shen, L., Cradle-to-grave life cycle assessment of single-use cups made from PLA, PP, and PET, *Resources, Conservation & Recycling*, vol. 169, no. 105508, 2021, Available: <https://doi.org/10.1016/j.resconrec.2021.105508>.
- Oliveira, J., Almeida, P. L., Sobral, R. G., Lourenço, N. D., and Gaudêncio, S. P., Marine-derived actinomycetes: Biodegradation of plastics and formation of PHA bioplastics—A circular bioeconomy approach, *Marine Drugs*, vol. 20, no. 12, 2022, Available: <https://doi.org/10.3390/md20120760>.
- Pereira, A. P. dos S., Silva, M. H. P. da, Lima Jr., É. P., and Tommasini, F., Processing and characterization of PET composites reinforced with geopolymers concrete waste, *Materials Research*, vol. 20, 2017, Available: <https://doi.org/10.1590/1980-5373-mr-2017-0734>.
- Phelan, A. (Any), Meissner, K., Humphrey, J., and Ross, H., Plastic pollution and packaging: Corporate commitments and actions from the food and beverage sector, *Journal of Cleaner Production*, vol. 331, 2022, Available: <https://doi.org/10.1016/j.jclepro.2021.129827>.

- Pomponi, F., Li, M., Saint, R., Lenzen, M., and D'Amico, B., Environmental benefits of material-efficient design: A hybrid life cycle assessment of a plastic milk bottle, *Sustainable Production and Consumption*, vol. 30, pp. 1044–1052, 2022, Available: <https://doi.org/10.1016/j.spc.2022.01.028>.
- Smith, B. C., Espectroscopía infrarroja de polímeros, VIII: Poliésteres y la regla de tres, *Spectroscopy*, vol. 37, no. 10, pp. 25-28, 2022, Available: <https://doi.org/10.56530/spectroscopy.ta9383e3>.
- Socrates, G., *Infrared and Raman Characteristic Group Frequencies: Tables and Charts*, 3rd Edition, John Wiley & Sons, 2001.
- Soong, Y. H. V., Sobkowicz, M. J., and Xie, D., Recent advances in biological recycling of polyethylene terephthalate (PET) plastic wastes, *Bioengineering*, vol. 9, no. 3, 2022, Available: <https://doi.org/10.3390/bioengineering9030098>.
- Suarez, A., Ford, E., Venditti, R., Kelley, S., Saloni, D., and Gonzalez, R., Rethinking the use of bio-based plastics to accelerate the decarbonization of our society, *Resources, Conservation and Recycling*, vol. 186, 2022, Available: <https://doi.org/10.1016/j.resconrec.2022.106593>.
- Venkatesulu, B., Srinivas, K., and Banerjee, A., Synthesis and characterization of novel polymers containing carbonyl bonds, *Polymers*, vol. 16, no. 8, pp. 1062, 2024, Available: <https://doi.org/10.3390/polym16081062>.
- Zeus, UV properties of plastics: Transmission and resistance, *RESINATE (Special Edition)*, October 2019, Available: <https://www.zeusinc.com/wp-content/uploads/2019/10/RESINATE-SE-UV-Props-Of-Plastics-Zeus.pdf>

Acknowledgements

The authors would like to express their gratitude to the laboratories of the University of Lima for their invaluable technical support and resources, which were instrumental in conducting this research. We also extend our sincere thanks to GS Company for generously providing the bottles and critical information that significantly contributed to the successful completion of this study.

Biographies

Camila Canturín is an outstanding Industrial Engineering student at the University of Lima, consistently ranked in the top 10% of her class since 2020. She has shown a strong commitment to continuous learning and technical skill development, complementing her academic studies with practical, hands-on professional experience. She currently works as a Commercial Management Intern in the Non Foods, Home Appliances division at Tottus, where she has developed essential skills in commercial management and data analysis. In addition, since 2023, she has been interning at Inca Rail S.A. in Commercial Management and Revenue Management, gaining experience in dynamic pricing analysis, the preparation of quotations, and strategic project oversight. Her professional training includes a Macros and Visual Basic course at the University of Lima, enhancing her skills in process automation and data analysis. She is proficient in Ms Office, Advanced Excel, SQL, and specialized software such as Power BI, Inventor, Visio, and Arena. In terms of languages, she holds an advanced level of English, certified by the First Certificate in English (FCE) from the University of Cambridge, and an intermediate level of French, certified by the B1 from the Centre International d'Études Pédagogiques. She has also participated in extracurricular activities, including being a semifinalist in the Divergencias debate competition and engaging in volunteer work in Amazonian communities.

Alessandra Rojas is an Industrial Engineering student at the University of Lima, ranked in the top 10% of her class since 2020. She has developed strong expertise in process optimization, supply chain management and operations planning, supported by practical experience in key industries. About her work experience, at Industria Textil Amazonas S.A.C., she improved inventory accuracy and developed procedures for purchasing and maintenance. Later, at L & S Consulting S.A.C., she led staffing initiatives for the Partner Digital project that expanded izipay's network by 51.37% and optimized workflows, reducing operational queries by 30%. Alessandra is certified in solid waste management and circular economy, and proficient in Excel, Power BI, and SAP. She holds a Cambridge First Certificate in English (FCE), certifying her at a B1 level, which complements her technical skills and enables her to perform effectively in diverse environments. Focused on sustainable solutions, she aims to enhance process efficiency and drive innovation in industrial operations.

Rafael Villanueva is an accomplished industrial engineer with over four decades of expertise in operations management and process engineering within the food and manufacturing sectors. He earned his Industrial Engineering

degree from Universidad de Lima in 1982 and later pursued a Master of Science in Food Science at Kansas State University in 1991, further enhancing his proficiency in optimizing production processes in the food industry. Villanueva began his career as Production Manager at Kraft Foods Peru, where he spent 11 years driving continuous improvement initiatives, overseeing quality control, and optimizing the supply chain, with a strong emphasis on implementing efficient production systems. He then held the same position at Molitalia, where he managed large-scale operations for nearly five years, applying Lean Manufacturing methodologies to enhance productivity and minimize waste. Since 2011, he has held the role of Operations Manager at Anita Food, where he has been responsible for overseeing the end-to-end production chain, ensuring operational efficiency through strategic resource management, the integration of advanced technologies, and strict adherence to quality and food safety standards. Simultaneously, Villanueva has served as an Associate Professor at Universidad de Lima since 1982, where he plays a vital role in shaping future industrial engineers, particularly in the fields of operations management, technology transfer, and industrial project development. His technical expertise and leadership have made him a distinguished figure in both industry and academia